ISSN 1674-1056
http://cpb.iphy.ac.cn
http://iopscience.iop.org/cpb
中国物理 B
Chinese Physics
中国物理 Chinese Physics B

Li adsorption on monolayer and bilayer MoS_2 as an ideal substrate for hydrogen storage

Cheng Zhang(张诚), Shaolong Tang(唐少龙), Mingsen Deng(邓明森), Youwei Du(都有为)
Citation: Chin. Phys. B . 2018, 27(6): 066103. **doi:** 10.1088/1674-1056/27/6/066103

Journal homepage: http://cpb.iphy.ac.cn; http://iopscience.iop.org/cpb

What follows is a list of articles you may be interested in

Structural, magnetic properties, and electronic structure of hexagonal FeCoSn compound

Yong Li(李勇), Xue-Fang Dai(代学芳), Guo-Dong Liu(刘国栋), Zhi-Yang Wei(魏志阳), En-Ke Liu(刘恩克), Xiao-Lei Han(韩小磊), Zhi-Wei Du(杜志伟), Xue-Kui Xi(郗学奎), Wen-Hong Wang(王文洪), Guang-Heng Wu(吴光恒)
Chin. Phys. B . 2018, 27(2): 026101. **doi:** 10.1088/1674-1056/27/2/026101

First-principles calculations of structure and elasticity of hydrous fayalite under high pressure

Chuan-Yu Zhang(张传瑜), Xu-Ben Wang(王绪本), Xiao-Feng Zhao(赵晓凤), Xing-Run Chen(陈星润), You Yu(虞游), Xiao-Feng Tian(田晓峰)
Chin. Phys. B . 2017, 26(12): 126103. **doi:** 10.1088/1674-1056/26/12/126103

Stability and mechanical properties of various Hf-H phases:A density-functional theory study

Wei Xiao(肖伟), Lu Sun(孙璐), Shu-Hui Huang(黄树晖), Jian-Wei Wang(王建伟), Lei Cheng(程磊), Li-Gen Wang(王立根)
Chin. Phys. B . 2017, 26(10): 106103. **doi:** 10.1088/1674-1056/26/10/106103

Effects of pressure on structural, electronic, and mechanical properties of *α*, *β*, and *γ* uranium

Hui-Jie Zhang(张慧杰), Shi-Na Li(李世娜), Jing-Jing Zheng(郑晶晶), Wei-Dong Li(李卫东), Bao-Tian Wang(王保田)
Chin. Phys. B . 2017, 26(6): 066104. **doi:** 10.1088/1674-1056/26/6/066104

High volumetric hydrogen density phases of magnesium borohydride at high-pressure: A first-principles study

Fan Jing, Bao Kuo, Duan De-Fang, Wang Lian-Cheng, Liu Bing-Bing, Cui Tian
Chin. Phys. B . 2012, 21(8): 086104. **doi:** 10.1088/1674-1056/21/8/086104

Li adsorption on monolayer and bilayer MoS_2 as an ideal substrate for hydrogen storage*

Cheng Zhang(张诚)[1,2], Shaolong Tang(唐少龙)[2,†], Mingsen Deng(邓明森)[3,‡], and Youwei Du(都有为)[2]

[1] School of Physics and Electronic Science, Guizhou Normal University, Guiyang 550001, China

[2] Department of Physics, Nanjing University, Nanjing 210093, China

[3] Guizhou Provincial Key Laboratory of Computational Nano-material Science, Guizhou Education University, Guiyang 550018, China

(Received 16 January 2018; revised manuscript received 2 March 2018; published online 10 May 2018)

Based on the first-principles plane wave calculations, we show that Li adsorbed on monolayer and bilayer MoS_2 forming a uniform and stable coverage can serve as a high-capacity hydrogen storage medium, and Li-coated MoS_2 can be recycled by operations at room temperature due to Li having strength binding, big separation and is stable against clustering. The full Li coverage MoS_2 system ($2*2$ hexagonal MoS_2 supercell) can reach up to eight H_2 molecules on every side, corresponding to the gravimetric density of hydrogen storage up to 4.8 wt% and 2.5 wt% in monolayer and bilayer MoS_2, respectively. The adsorption energies of hydrogen molecules are in the range of 0.10eV/H_2–0.25 eV/H_2, which are acceptable for reversible H_2 adsorption/desorption near ambient temperature. In addition, compared with light metals decorated low dimension carbon-based materials, the sandwiched structure of MoS_2 exhibits the greatly enhanced binding stability of Li atoms as well as slightly decreased Li-Li interaction and thus avoids the problem of metal clustering. It is interesting to note that the Li atom apart from the electrostatic interaction, acts as a bridge of hybridization between the S atoms of MoS_2 and adsorbed H_2 molecules. The encouraging results show that such light metals decorated with MoS_2 have great potential in developing high performance hydrogen storage materials.

Keywords: MoS_2, Li anchoring, hydrogen storage, first-principles

PACS: 61.46.–w, 63.20.dk, 88.30.R– **DOI:** 10.1088/1674-1056/27/6/066103

1. Introduction

Due to the problems of global warming and limited oil supply, there is an urgent need for alternative clean energy sources in place of traditional fossil fuels. Hydrogen, as one of the most abundant elements in the world, has been considered as an ideal clear energy carrier due to its lightweight, nonpolluting, highly efficient, and easily derived attributes.[1,2] However, many technical challenges need to be overcome for a wide application of hydrogen. For instance, it remains challenging to develop cost-effective, safe, and reliable technologies for compact hydrogen storage. Traditionally, compact hydrogen storage requires hydrogen gas to be physically stored either in a compressed gas state or in a liquid state, and this will lead to a serious safety problem. Therefore, finding and developing an optimal medium for safe and efficient hydrogen storage has become essential and meaningful in scientific and engineering applications.

For application, a desirable hydrogen storage system must have a high gravimetric and volumetric density, and be low cost and safe. Recently, the carbon-based nanomaterials, such as graphene,[3–5] carbon nanotube,[6,7] and carbon fullerenes,[8,9] have drawn sufficient interest owing to the possibility of reversibility, fast kinetics, and large surface area to volume ratio. However, it is still a challenge to fabricate carbon-based nanomaterials with high hydrogen storage capacity because the interaction between hydrogen molecules and pristine carbon nanostructures is too weak to be useful for practical hydrogen storage. To date, more theoretical and experimental studies have been devoted to increase their chemical activity by decorating the carbon nanostructures with metal atoms, such as alkali metal,[10,11] alkaline-earth metal,[12,13] and transition metal.[14–16] Metal atoms are dispersed onto such carbon nanostructures through different experimental conditions.[17–19] Specifically, since the cohesive energies of transition metal ($\sim$ 4 eV) are bigger than the binding energies of transition metal ($\sim$ 3 eV) on carbon nanostructures, thus they are prone to clustering, which can greatly reduce the capacity of hydrogen storage.[20] In addition, alkali metal can be adsorbed stabilized and uniformly on carbon nanostructures due to their much smaller cohesive energy, but the binding energy of a hydrogen molecule is less than that of transition metal decorated carbon-based nanostructures.[21–23] Then, there are two major problems that remained unsolved, which prevent practical applications of these carbon-based

*Project supported by the National Key Basic Research Program of China (Grant No. 2012CB932304), the National Natural Science Foundation of China (Grant No. 21763007), the Innovation Team Foundation of the Education Department of Guizhou Province, China (Grant No. [2014]35), and the Key Laboratory of Low Dimensional Condensed Matter Physics of Higher Educational Institution of Guizhou Province, China (Grant No. [2016]002).

†Corresponding author. E-mail: tangsl@nju.edu.cn

‡Corresponding author. E-mail: deng@gznc.edu.cn

© 2018 Chinese Physical Society and IOP Publishing Ltd

nanomaterials: (i) the binding energy of H_2 molecular is too small (for application, the binding energy of per H_2 molecular on these materials should in the range of 0.1 eV–0.25 eV for sufficient storage[24]); (ii) another important issue is metal adsorbate clustering.[25]

The monolayer MoS_2 is made of a honeycomb sheet of molybdenum atoms covalently sandwiched between two honeycomb sheets of sulphur atoms, which has attracted a great deal of attention due to its sandwiched structure and intriguing properties. Bilayer MoS_2 is composed of vertically stacked monolayers of MoS_2 with 0.65-nm distance, which are weakly interacting layers held together by van der Waals interactions.[26] However, the interlayer van der Waals interactions between the two monolayers can notably affect the electronic properties of the two-dimensional nanomaterial.[27–30] In this study, we present systematic theoretical studies on the structures and properties of different Li coverage monolayer and bilayer MoS_2. We also consider the diffusion barrier for Li atom moved in the setting path in the case of full Li coverage. Besides, we analyze the adsorption configurations and energetics of H_2 molecules adsorbed on those systems. Our main concerns are as follows: i) what are the adsorption configurations and energetics of Li atoms on monolayer and bilayer MoS_2; ii) how do the Li atoms affect H_2 molecules adsorption on monolayer and bilayer MoS_2? To answer these questions, we investigate the electronic properties of Li-coated monolayer and bilayer MoS_2.

Computational details: Our calculations are performed using density-functional theory (DFT) through the Vienna ab initio simulation package (VASP) code.[31] The general gradient approximation (GGA) parameterized by Perdew, Burke, and Ernzerhof (PBE)[32] is used as the exchange–correlation functional, and the projector augmented-wave (PAW)[33,34] method is used to describe the ions–electro interaction. A kinetic energy cutoff 500 eV for the plane-wave basis, and the Brillouin zone is sampled in k-space using the Monkhorst–Pack scheme by $6\times6\times1$ for the 2*2 hexagonal MoS_2 supercell. In the structural optimization, convergence of the Hellmann–Feynman forces is set less than 0.01 eV/Å per atom and the vacuum region of greater than 20 Å to avoid artificial interactions in the Z direction.

To find the most stable adsorption site for Li atoms among the probable adsorption sites in Li-coated MoS_2 systems, the specific Li atoms are placed on the Mo top site (A), the S top site (B), and the hexagonal center site (C), which are not established randomly but build on the basis of the structure of the honeycomb sheet and the rule for decorating metals. In our simulation, the Li atoms are placed randomly onto the MoS_2 with a perpendicular distance of 2.0 Å to 4.0 Å. After full structures optimization, the average binding energy of the n Li atoms on MoS_2 is defined as

$$E_{\mathrm{bind,Li}} = [E(\mathrm{MoS_2}) + nE(\mathrm{Li}) - E(\mathrm{Li/MoS_2})]/n, \quad (1)$$

where n indicates the number of Li atoms, $E(\mathrm{MoS_2})$, $E(\mathrm{Li})$, and $E(\mathrm{Li/MoS_2})$ are the total energies of pure MoS_2, a free Li atom, and the Li-coated MoS_2 systems, respectively.

In order to optimize atomic structures of H_2 molecules adsorbed on Li-coated MoS_2 systems, H_2 molecules are placed randomly onto the Li atoms with a perpendicular distance of 2.0 Å to 4.0 Å. The initial bond length $d_{\mathrm{H-H}}$ in H_2 molecules is set at 0.70 Å (0.70 Å in the gas phase). After full structures optimization, the average adsorption energy of the H_2 molecule ($E_{\mathrm{ads,H_2}}$) is defined as

$$E_{\mathrm{ads,H_2}} = [E(\mathrm{Li/MoS_2}) + nE(\mathrm{H_2}) - E(\mathrm{H_2@Li/MoS_2})]/n, \quad (2)$$

where n indicates the number of H_2 molecules, $E(\mathrm{Li/MoS_2})$, $E(\mathrm{H_2})$, and $E(\mathrm{H_2@Li/MoS_2})$ are the total energy of the Li-coated MoS_2 system, the pure H_2 molecular system, and the H_2 adsorbed on Li-coated MoS_2 system, respectively. After the full structures optimization, the adsorption energy of the n-th hydrogen molecule $E_{\mathrm{ads},n\text{-th H}_2}$ is calculated by using

$$E_{\mathrm{ads},n\text{-th H}_2} = E_{n-1}^{\mathrm{H_2\,on\,Li/MoS_2}} + E_{\mathrm{H_2}} - E_{n}^{\mathrm{H_2\,on\,Li/MoS_2}}, \quad (3)$$

where $E_{n-1}^{\mathrm{H_2\,on\,Li/MoS_2}}$ is the energy of the $(n-1)$ H_2 molecules adsorbed on the Li-coated MoS_2 system, $E_{n}^{\mathrm{H_2\,on\,Li/MoS_2}}$ is the energy of the n H_2 molecules adsorbed on the Li-coated MoS_2 system, and $E_{\mathrm{H_2}}$ is the energy of the H_2 molecular system.

In this work, we also focus on the hydrogen molecule dissociates on both sides of Li-coated MoS_2 by finite-temperature *ab initio* molecular dynamics simulations. The *ab initio* molecular dynamics simulations are performed by normalizing the velocities of the ions at 300 K (room temperature) and 350 K in 1000 times steps, as implemented in the VASP code. The duration of time steps are intentionally taken as 1 fs, which is relatively longer for a molecular dynamics calculation.

2. Results and discussion

First, the density functional theory calculations show that the monolayer MoS_2 is a semiconductor with a direct bandgap of 1.60 eV at the K point. However, the bilayer MoS_2 is a semiconductor with an indirect bandgap of 1.40 eV, the valence maximum and the conduction band minimum occur at the Γ point and K point (see Fig. 1(c)), respectively, in agreement with a previous calculation.[35] Next, we examine the adsorption site of a single Li atom adsorption on the monolayer MoS_2. Three high-symmetry sites are tested, on the Mo top site (A), the S top site (B), and the hexagonal center site (C). After full structures optimization, a single Li atom prefers to adsorb strongly at the A site, with a binding energy of 2.35 eV

and a distance of 2.90 Å between the Mo and Li atoms. It is very interesting to note that after full structures optimization the Li atom will move to the A site even if the Li atom is placed onto the S atom at first, suggesting that the Li atom adsorbed on the S top site is unstable, just as in a previous result.[36] On the bilayer MoS_2, the Li atom is also more stable on the A site, and the binding energy and the Li–Mo distance are nearly the same as those in the monolayer MoS_2. For comparison, we also calculate the bulk cohesive energies of Li. The binding energy of Li on the A site is larger than that of the Li bulk cohesive energies (1.89 eV), suggesting that clustering of Li atoms might be seriously hindered by the high binding energy.

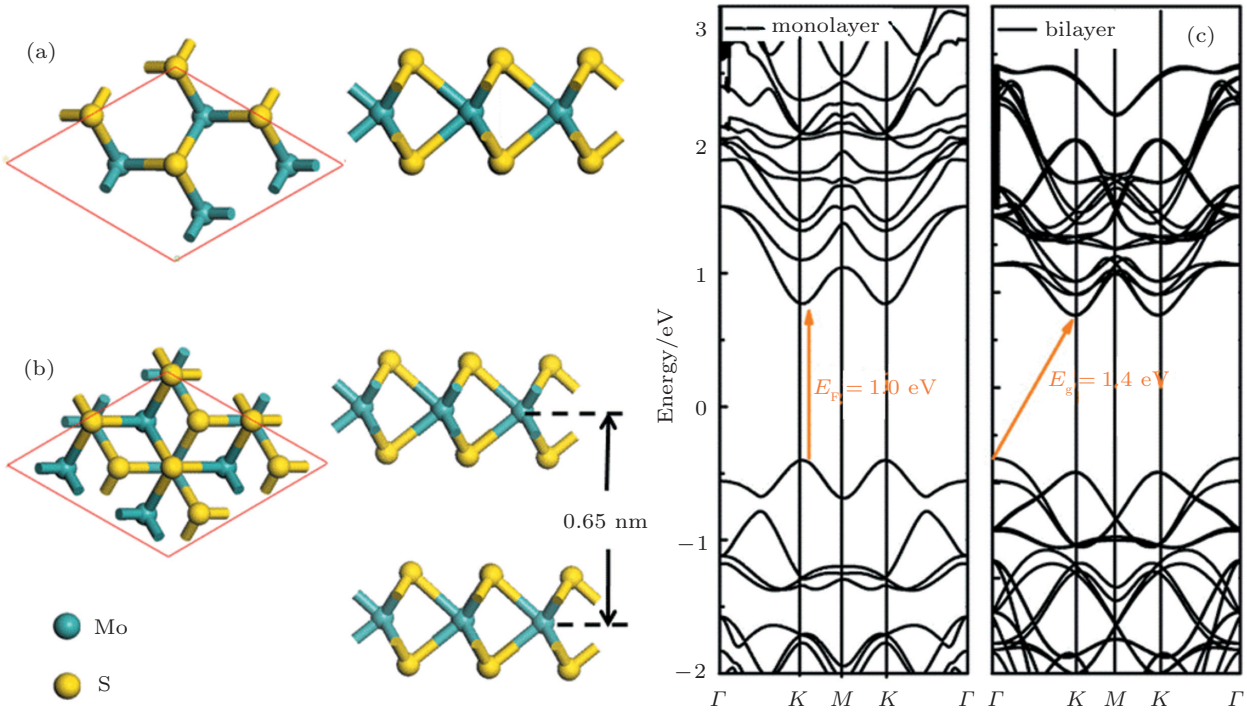


Fig. 1. (color online) Top and side view of typical atomic structures of monolayer (a) MoS_2 and (b) bilayer MoS_2, the Mo and S atoms are represented by olive and yellow spheres, respectively; (c) band structures of monolayer MoS_2 and bilayer MoS_2, direct band occurs at the K point in monolayer MoS_2, and indirect band transition occurs between the valence band maximum at Γ point and the conduction band minimum at K point in bilayer MoS_2.

To achieve optimized hydrogen storage capacity, the Li-coated MoS_2 system should have a larger number of Li atoms forming a uniform and stable coverage due to the hydrogen molecule being generally absorbed near the Li atoms.[37] Thus, we discuss the structures and electronic properties of Li-coated MoS_2 with high Li coverage cases by adsorbing two, three, and four Li atoms on MoS_2 (there are a total of four stable adsorption sites in one side of the $2*2$ hexagonal MoS_2 supercell according to our calculations). We defined Θ as the ratio of the number of adsorbed Li atoms to the total adsorption sites. Thus the one, two, three, and four adsorption Li atoms correspond to Li coverage of $\Theta = 0.25$, $\Theta = 0.50$, $\Theta = 0.75$, and $\Theta = 1.0$, respectively. However, it should be noted that the sandwich structure of MoS_2 can adsorb Li atoms on both sides, in which Li atoms bind to the S atoms of MoS_2 and exhibit as well separated compared with that in low-dimension carbon-based materials. As expected, when one Li is adsorbed on one side of monolayer MoS_2, the second Li atom prefers to be adsorbed on the same Mo top site on the other side. The same phenomenon also exists in bilayer MoS_2, the second Li atom prefers to be adsorbed on the opposite Mo top site in the other MoS_2 sheet. We believe that it is possible due to the atomic structures of these Li-coated MoS_2 with high symmetry, which is in agreement with previous results.[38] By comparing the total energy of more Li atoms adsorption on one side of MoS_2, we find that Li atoms prefer to be adsorbed on the nearest Mo top sits in the high Li coverage case ($\Theta = 0.50$, and $\Theta = 0.75$) no matter whether in monolayer and bilayer MoS_2. The optimized geometric structures, the average Mo–Li distance, and adsorption energy per Li atom for different Li coverage monolayer MoS_2 are shown in Fig. 2(a). Our results show that the average Mo–Li distance is increased as the Li coverage increases, suggesting that the average adsorption energy of Li atom decreases with the increase of the Θ. It is worth noticing that the average adsorption energy of per Li atom even in the full Li coverage case is still larger than the Li bulk cohesive energies, suggesting that the decorated Li atom highly prefers being on the A site rather than forming metal clustering.

In the case of high coverage Li-coated MoS_2, another important question that should be asked is whether the metal atoms are normally highly mobile and tend to form clusters on the MoS_2 sheet. To clearly analyze the issue of Li clustering, we have calculated the diffusion barrier for one Li atom moved in the direction of the set path in full Li coverage mono-

layer MoS_2. As a Li atom at the initial position (the optimized structure) is moved in the direction of the arrow, its z coordinate is optimized (x coordinate and y coordinate are fixed according to the basis of the honeycomb sheet and the rule for diffusion pathway). The remaining three Li atoms are fully relaxed. Our calculations show that during the process of the first Li moving, the other three Li atoms are pushed in the same direction under Coulomb repulsion. Finally, all Li atoms are adsorbed on the nearest Mo top sits, where Li atoms have a stability configuration. That is, the clustering of adsorbed Li atoms is prevented by the Coulomb repulsion. The variation of the atomic geometries and energies is the first Li moving in the direction of the arrow, as is shown in Fig. 2(b).

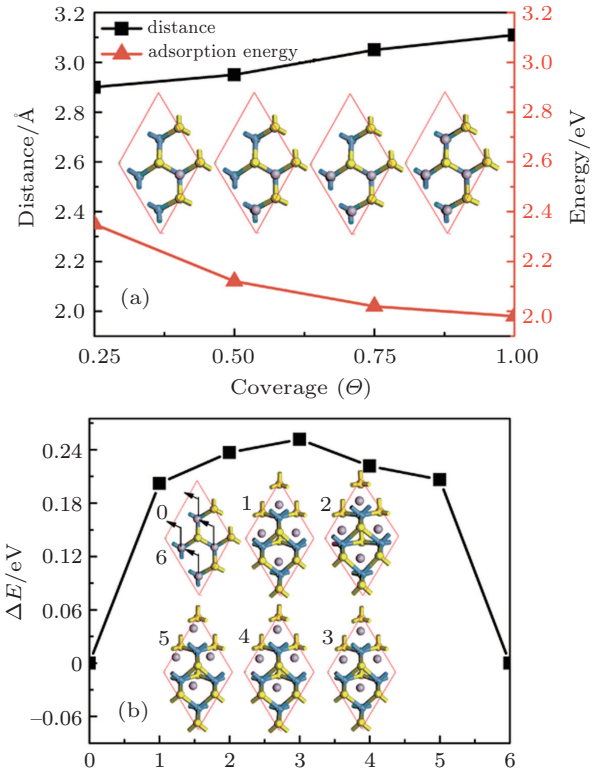


Fig. 2. (color online) (a) Average Mo–Li distances and adsorption energies of per Li atom for different Li coverage ($\Theta = 0.25$, $\Theta = 0.50$, $\Theta = 0.75$, and $\Theta = 1.0$) in monolayer MoS_2; (b) the variation of the atomic geometries and energies as one Li atom moving in the direction of the arrow in full Li coverage monolayer MoS_2.

According to the variation of energies during the process (the maximum $\Delta E = 0.24$ eV), it is believe that Li atoms forming a cluster by moving on the MoS_2 sheet is prevented by the greater potential barrier.[39] For comparison, we have considered another Li atom adsorption on full Li coverage monolayer MoS_2. The fifth Li atom is placed randomly on the monolayer MoS_2 with a perpendicular distance of 2.0 Å to 4.0 Å. After full structure optimization, the fifth Li atom is adsorbed onto the previous four Li atoms forming metal clustering (see Fig. S1 in Appendix A: the Supporting Information). The binding energy between the fifth Li atom and the previous four Li atoms is about 2.12 eV, and the bonds length of Li–Li are about 3.27 Å. There is no doubt that the Li adsorbate clustering will severely limit the hydrogen storage capacity because the fifth Li atom is able to occupy the adsorption sites for H_2 molecules, which is consistent with the previous report.[40] Therefore, to achieve the highest hydrogen storage capacity, the amount of adsorbed Li atoms should be controlled as any excess loading will delay the adsorption sites for H_2 molecules thus sacrificing hydrogen storage capacity.

Now we investigate the interaction between Li-coated MoS_2 systems and H_2 molecules. We first consider $\Theta = 0.25$ Li coverage on one side of the MoS_2 system. In our calculation, we place one hydrogen molecule randomly onto the Li atom with a perpendicular distance of 2.0 Å to 4.0 Å. After optimization calculations, the first H_2 molecule is adsorbed on the high-symmetry sites (on the top of the hexagonal center site) and lies tilted towards the Li atom. The adsorption energy and distance between Li atom and H_2 molecule are 0.21 eV and 2.01 Å, respectively, and the H–H bond is expanded 0.765 Å. Then we increase the number of adsorbed H_2 molecules to search for the maximum number of H_2 molecules adsorbed on the Li-coated MoS_2 system. It is found that whatever the initial H_2 molecules locations are near the Li atom, the seventh H_2 molecule prefers to move away from the Li atom and cannot be adsorbed. More interestingly, in the case of the fourth H_2 molecules adsorption, due to the symmetry of the charge configuration of the Li-coated MoS_2 systems, they tend to move quite far away from Li with 2.52 Å, almost on the S top site. Intuitively, the reason why there is a long distance between Li atom and the fourth H_2 molecule is that there is no available space for a H_2 molecule in the first layer occupied by the previous three H_2 molecules. The fifth and sixth H_2 molecules are adsorbed about 2.52 Å above the Li atom and form the second-layer H_2 molecules with the fourth H_2 molecule. The optimized atomic structure for the configuration with the number of maximally adsorbed hydrogen molecules on the $\Theta = 0.25$ Li coverage one side of the MoS_2 system are given in Fig. 3(a). In bilayer MoS_2, six H_2 molecules can be adsorbed. The atomic structures for the configuration are nearly as the same as those in monolayer MoS_2. As shown in Fig. 3(c), six H_2 molecules are adsorbed on symmetry sites, which lie tilted towards the Li atom, and form two layers configuration. Furthermore, the corresponding adsorption energetics, distances between Li atom and H_2 molecule are listed in Table 1.

Then, we study H_2 molecules adsorbed on $\Theta = 0.25$ Li covering both sides of the MoS_2 system. After full structural optimization, the pairing of Li atoms are located at the opposite sides of the MoS_2 sheet with distances of 5.75 Å and 13.01 Å in monolayer and bilayer MoS_2, respectively. Figures 3(b) and 3(d) show that every Li atom can adsorb up to six H_2 molecules in $\Theta = 0.25$ Li coverage on both sides of the MoS_2 system. As expected, the average H_2 binding energy and distances between H_2 and Li atoms exhibit as being similar to those of $\Theta = 0.25$ Li covering one side of MoS_2. In addition, the corresponding adsorption energetics, distances

between Li atom and H_2 molecule are listed in Table 1. Furthermore, in all of those adsorption structures, there is only a small change in H_2 bond lengths as about 0.75 Å because the interaction between H_2 molecules and Li-coated MoS_2 system mainly exhibit characteristics of physisorption.

Table 1. The adsorption energy of the n-th H_2 molecule ($E_{ads,n-th\,H_2}$ (in unit eV)), average adsorption energy per H_2 molecule (E_{ads,H_2} (in unit eV)), distance between Li atom and H_2 molecule (d_{Li-H_2} (in unit Å)) for different number of H_2 molecule adsorption on one side $\Theta = 0.25$ Li coverage MoS_2 systems.

The n-th H_2	Li-coated system	$E_{ads,n-th\,H_2}$	E_{ads,H_2}	d_{Li-H_2}
1	monolayer MoS_2	0.21	0.21	2.01
	bilayer MoS_2	0.20	0.20	2.02
2	monolayer MoS_2	0.20	0.21	2.02
	bilayer MoS_2	0.19	0.20	2.04
3	monolayer MoS_2	0.19	0.20	2.04
	bilayer MoS_2	0.17	0.19	2.06
4	monolayer MoS_2	0.14	0.19	2.52
	bilayer MoS_2	0.13	0.17	2.72
5	monolayer MoS_2	0.13	0.17	2.53
	bilayer MoS_2	0.13	0.16	2.72
6	monolayer MoS_2	0.12	0.16	2.53
	bilayer MoS_2	0.11	0.16	2.72

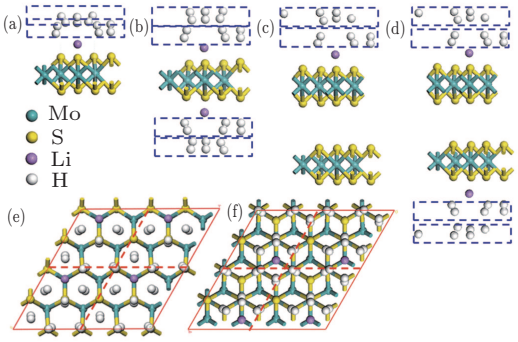


Fig. 3. (color online) Optimized atomic geometries for the maximum number of hydrogen molecules adsorbed on $\Theta = 0.25$ Li coverage one side and both sides of the MoS_2 system. Hydrogen molecules are formed in two layer structures. To elaborate further on the configuration of the adsorbed hydrogen molecules, the top view of 6 hydrogen molecules adsorbed on $\Theta = 0.25$ Li coverage MoS_2 $4*4$ supercell are shown in the bottom panel. Top view of 6 hydrogen molecules adsorbed on $\Theta = 0.25$ Li coverage (e) monolayer and (f) bilayer MoS_2, respectively.

Then the next question would be whether the hydrogen storage capacity is increased with the number of adsorbed Li atoms increases. To address this question, we analyze the stable structure and adsorption energy of H_2 molecules adsorbed on a high-coverage Li–MoS_2 system, specifically for the full Li coverage case. We choose an initial geometry, where H_2 molecules are placed randomly above the Li atoms with a perpendicular distance of 2.0 Å to 4.0 Å. Step by step, we add additional hydrogen molecules close to the Li atoms, where the hydrogen molecules adsorbed on $\Theta = 1.0$ Li coverage on both sides monolayer and bilayer MoS_2 systems are fully optimized. Finally, a total of 16 H_2 molecules can be adsorbed onto the surface of the $\Theta = 1.0$ Li coverage MoS_2 systems, corresponding to the gravimetric density of hydrogen storage up to 4.8 wt% and 2.5 wt% in monolayer and bilayer MoS_2, respectively. The fully relaxed structures of 16 H_2 molecules adsorbed on the Li-coated MoS_2 system are shown in Fig. 4. The 16 H_2 molecules are adsorbed on the high-symmetry sites (on the top of Mo atoms and S atoms) and are perpendicular to the plane of the MoS_2 sheet. We note that all H_2 molecules are formed in two layer structures, which is the same as those in $\Theta = 0.25$ Li coverage MoS_2 systems. Furthermore, the adsorption energetics, distances between Li atom and H_2 molecule for different number of H_2 molecule adsorption on one side of $\Theta = 1$ Li coverage MoS_2 systems are very similar to those of H_2 molecule adsorption on both sides of $\Theta = 1$ Li coverage MoS_2 systems, and details of the results are listed in Table 2. For comparison, we have investigated the atomic structures of the maximal number of adsorbed H_2 molecules for $\Theta = 0.5$ and $\Theta = 0.75$ Li coverage monolayer MoS_2 systems, suggesting that six and seven H_2 molecules can be adsorbed on $\Theta = 0.5$ and $\Theta = 0.75$ Li coverage monolayer MoS_2, respectively (see Fig. S4 in Appendix A: the Supporting Information).

Table 2. The adsorption energy of the n-th H_2 molecule ($E_{ads,n-th\,H_2}$ (in unit eV)), average adsorption energy per H_2 molecule (E_{ads,H_2} (in unit eV)), distance between Li atom and H_2 molecule (d_{Li-H_2} (in unit Å)) for different number of H_2 molecule adsorption on one side $\Theta = 1$ Li coverage MoS_2 systems.

The n-th H_2	Li-coated system	$E_{ads,n-th\,H_2}$	E_{ads,H_2}	d_{Li-H_2}
1	monolayer MoS_2	0.25	0.25	1.96
	bilayer MoS_2	0.24	0.24	1.97
2	monolayer MoS_2	0.24	0.25	1.98
	bilayer MoS_2	0.23	0.24	2.04
3	monolayer MoS_2	0.23	0.24	2.04
	bilayer MoS_2	0.22	0.23	2.06
4	monolayer MoS_2	0.22	0.23	2.06
	bilayer MoS_2	0.21	0.22	2.07
5	monolayer MoS_2	0.18	0.22	2.83
	bilayer MoS_2	0.18	0.21	2.85
6	monolayer MoS_2	0.18	0.21	2.84
	bilayer MoS_2	0.17	0.20	2.86
7	monolayer MoS_2	0.17	0.21	2.88
	bilayer MoS_2	0.16	0.20	2.90
8	monolayer MoS_2	0.16	0.20	2.90
	bilayer MoS_2	0.15	0.19	2.93

Finally, in order to analyze the H_2 molecules dissociated on both sides of H_2 adsorption on the $\Theta = 1$ Li coverage monolayer MoS_2 system, we carry the process out for a 3-ps duration with a time step of 3 fs in the simulations at 300 K (room temperature) and 350 K. The snapshots for the simulation at 300 K are plotted in Fig. 5. It is clear that eight H_2 molecules are dissociated in the molecular form on both sides of Li-coated MoS_2, and all Li atoms still remain adsorbed on the MoS_2 sheet. The structure of MoS_2 can be sustained, while the bonding between adsorbed Li atoms and the MoS_2 sheet are weakened slightly. Interestingly, the dissociated H_2 molecules are in the atomic form when the simulation temperature increased to 350 K (see Fig. S5 in Appendix A: the Supporting Information), suggesting that the Li-coated MoS_2 is invalidated as potential hydrogen storage media at 350 K.

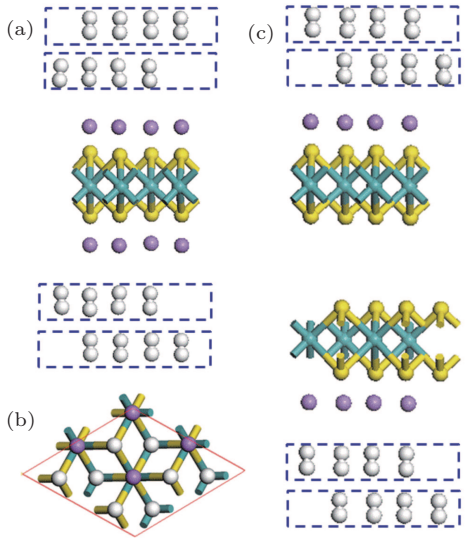


Fig. 4. (color online) Side (a) and top (b) view of 16 H_2 molecules adsorbed on $\Theta = 1.0$ Li coverage monolayer MoS_2; (c) side view of 16 H_2 molecules adsorbed on $\Theta = 1.0$ Li coverage bilayer MoS_2 (top view of 16 H_2 molecules adsorbed on $\Theta = 1.0$ Li coverage bilayer MoS_2 exhibit similar to those in Θ=1.0 Li coverage monolayer MoS_2).

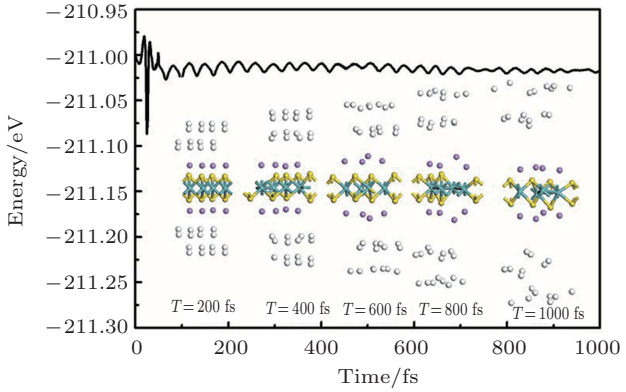


Fig. 5. (color online) Simulation snapshots of the hydrogen molecule dissociates on both sides of H_2 adsorption on $\Theta = 1$ Li coverage monolayer MoS_2 system with the simulation temperature set to 300 K.

To explain the adsorption mechanism, we have plotted the isosurfaces of deformation charge density and potential lineups of Li-coated MoS_2 systems, as shown in Figs. 4(a)–4(c). The deformation electronic density is defined as the total electronic density excluding those of isolated atoms. The red color corresponds to positive values (electron accumulation), and blue to the negative values (electron deletion). As shown in Figs. 6(a) and 6(b), it is obvious that there is a significant charge transfer from Li atoms to S atoms, which forms an electronic field along the z axis and enhances the polarization H_2 molecule adsorption. It is suggested that a possibility for H_2 molecule adsorption is due to the polarization mechanism.[41] Furthermore, it is worth noting that the average charge transfer from the Li atom to the MoS_2 sheet decreases with the increase of Li coverage in Li-coated MoS_2 systems due to the Coulomb repulsion between adsorbed Li atoms.[42] The Bader charge analysis shows that the charge transfer from the Li atom to the MoS_2 sheet is about $0.860e$ and $0.859e$ in $\Theta = 0.25$ Li coverage monolayer MoS_2 and bilayer MoS_2 systems, respectively. However, the average charge transfer in $\Theta = 1$ Li coverage monolayer MoS_2 and bilayer MoS_2 are only $0.411e$ and $0.409e$. Besides, the monolayer and bilayer MoS_2's energy-levels are shifted down due to the adsorption of Li atoms, as shown in Fig. 6(c). Our further investigation shows that the Pauli-exclusion principle and self-compensation effect play a critical role in the electron densities redistribution. The Li ($2S^1$) atom has one valence electron, so when Li atoms are close to the MoS_2 sheet, then the Li's outermost s-electrons with large radial electron density distribution will overlap with S ($3S^23P^4$) orbitals. It is thus the Pauli-exclusion interaction pushes the electrons back into both Li atoms and MoS_2 away from the interface.[43,44]

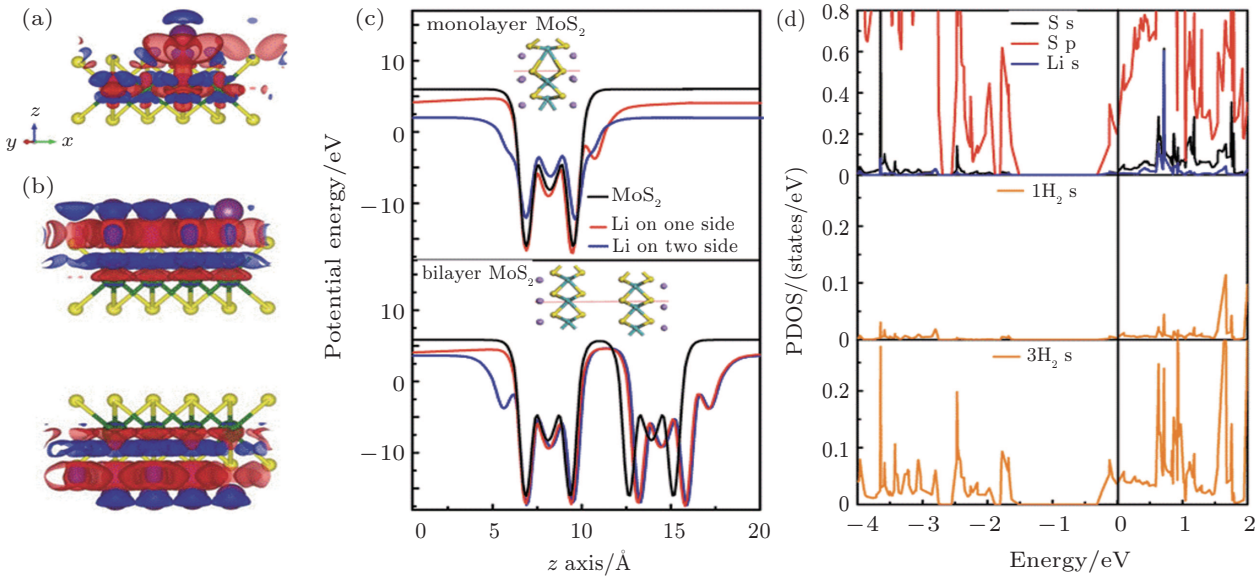


Fig. 6. (color online) The isosurface (2.0×10^{-3} e in Å^{-3}) of deformation electronic density of Li adsorbed (a) monolayer MoS_2 and (b) bilayer MoS_2; (c) potential diagrams of pure monolayer MoS_2, Li adsorbed on one side and both sides of monolayer MoS_2, pure bilayer MoS_2, Li adsorbed on one side and both sides of bilayer MoS_2; (d) the partial density of states of $\Theta = 0.25$ Li coverage on one side of monolayer MoS_2, one H_2 molecule adsorbed on one side of $\Theta = 0.25$ Li coverage MoS_2, and three H_2 molecules adsorbed on one side of $\Theta = 0.25$ Li coverage MoS_2, zero energy is set to the Fermi level.

To better understand the charge transfer and interaction between Li atoms and MoS_2 sheet, we also calculate the electronic dipole moment perpendicular to the MoS_2 sheet for different Li coverage on one side and both sides of monolayer and bilayer MoS_2. The dipole moment is defined as $\int (r - R_{\text{center}})\rho_{\text{ions+valence}} r\,\mathrm{d}^3 r$, where R_{center} is the charge density averaged over a plane that drops to a minimum, and we predict the charge distribution of the center by adding half of the lattice vector perpendicular to the plane where the charge density has a minimum. The dipole moments of Li coverage on both sides of monolayer and bilayer MoS_2 are almost zero because of the symmetry of the atomic configuration of the monolayer and bilayer MoS_2 along the z axis. However, the dipole moments of Li coverage on one side of monolayer and bilayer MoS_2 are very sensitive to the Li coverage. Compared with monolayer MoS_2, the Li-coated bilayer MoS_2 exhibited higher dipole moment under the same Li coverage, the biggest dipole moment of the bilayer MoS_2 is 1.3 Debye at the $\Theta = 0.25$ Li coverage. Surprisingly, the value of dipole moments of monolayer and bilayer MoS_2 are not in a monotonously increasing trend, with the Li coverage increased (see Fig. S2 in Appendix A: the Supporting Information).

Figure 6(d) shows the projected density of states (PDOS) for $\Theta = 0.25$ Li coverage monolayer MoS_2, one H_2 molecule adsorbed $\Theta = 0.25$ Li coverage MoS_2, and three H_2 molecules adsorbed $\Theta = 0.25$ Li coverage MoS_2. Due to the interaction with MoS_2 sheet, the 1s and 2s states of Li are split into lots of prominent peaks in the vicinity of -5.0 eV and 1.0 eV, respectively. The 2s peak lies approximately 0.6 eV above the Fermi level and is almost unoccupied, suggesting that most of Li($2s^1$) electrons transfer from the Li atom to the closer MoS_2 sheet. It can be clearly seen that there is strong hybridization between the S($3p^3$) orbitals and the H_2 molecule state at about -5.5 eV and 2.3 eV in three H_2 molecules adsorbed $\Theta = 0.25$ Li coverage MoS_2. Thus, the Li atom apart from the electrostatic interaction acts as a bridge of hybridization between the H_2 molecule state and the S($3p^3$) orbitals of MoS_2, which plays an important role in the hydrogen molecules adsorption process.

We next analyse the sandwiched structure effect on the hydrogen adsorption and storage properties. Firstly, the sandwiched structure affects the binding between Li and S. Comparable with other 2D sheet materials, the Li on the Mo top site has strong interactions with the top honeycomb sheet of S atoms. Thus, the sandwiched structure enhances the stability of Li atoms. Secondly, the Mo atoms covalently sandwiched between S atoms drops the Li–Li repulsive interaction compared with 2D sheet materials, due to the bigger distances between the adjacent adsorption Li atoms. Finally, the 3p orbitals of the top honeycomb sheets of S atoms hybridize strongly with H_2 σ, σ^* orbitals, leading to strong adsorption with H_2 molecules. For this reason, the adsorbed Li atom acts as a bridge, which enhances the interaction between H_2 molecules and the MoS_2 sandwiched structure.

3. Conclusions

In conclusion, by first-principles calculation, we have studied the adsorption configurations and energetics of Li-coated monolayer and bilayer MoS_2 and H_2 molecules adsorbed on those system. Compared with graphene, Li has strength binding, big separation, and is stable against clustering on MoS_2, making Li-coated MoS_2 a great option for efficient hydrogen storage materials. Due to the Li atom being apart from the electrostatic interaction, it acts as a bridge of hybridization between the S atoms and the H_2 molecules; up to 16 H_2 molecules can be adsorbed on a $2*2$ suppercell of a full Li coverage MoS_2 system, corresponding to the gravimetric density of hydrogen storage up to 4.8 wt% and 2.5 wt% in monolayer and bilayer MoS_2, respectively. Furthermore, our MD simulations show that the Li-coated MoS_2 system can be recycled by operations at room temperature, suggesting significant potential applications in hydrogen storage technologies.

Acknowledgment

All the calculations are performed at Guizhou Provincial High-Performance Computing Center of Condensed Materials and Molecular Simulation in GZEU.

Appendix A: Supporting Information

Some of the supporting information are provided for help in understanding the present study in the following figures as shown in Figs. S1–S5.

The top and side view of the optimized atomic geometries for five Li atoms adsorbed on MoS_2 is shown in the following Fig. S1.

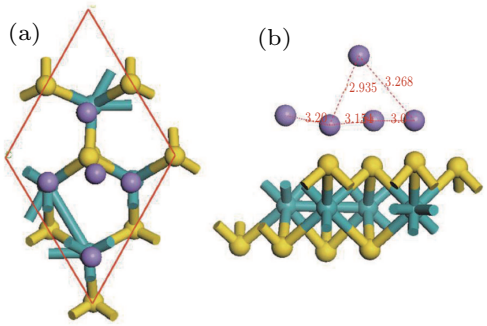


Fig. S1. (color online) Top and side view of the optimized atomic geometries for five Li atoms adsorbed on MoS_2. The distances between the Li atoms are listed. It can be clearly seen that the fifth Li atom is adsorbed on the top of the previous four Li atoms and forms metal clustering, which will reduce the number of adsorption hydrogen molecules.

The dipole moment of different Li coverages on one side of monolayer and bilayer MoS_2 is shown in Fig. S2.

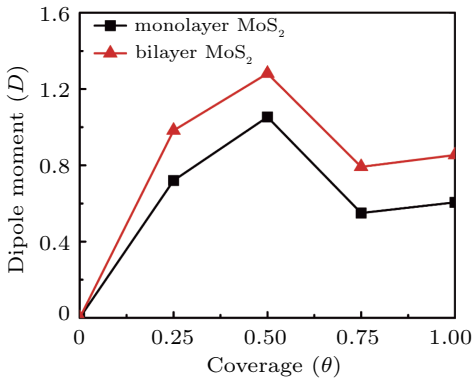


Fig. S2. (color online) The dipole moment of different Li coverages on one side monolayer and bilayer MoS_2.

The spin density map of the antiferromagnetic ground state on one side of $\Theta = 1.0$ Li coverage monolayer MoS_2 and 4 hydrogen molecules adsorbed on one side of $\Theta = 1.0$ Li coverage monolayer MoS_2 is shown in Fig. S3.

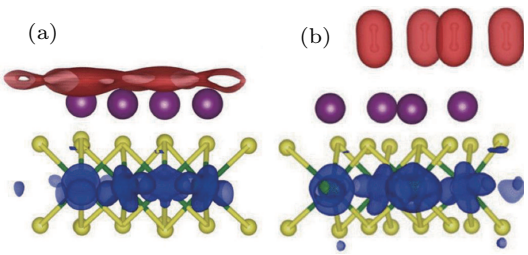


Fig. S3. (color online) The spin density (different between α-spin and β-spin density) map of the antiferromagnetic ground state on one side of $\Theta = 1.0$ Li coverage monolayer MoS_2 (a) and 4 hydrogen molecules adsorbed on one side of $\Theta = 1.0$ Li coverage monolayer MoS_2 (b). The red line: positive, blue line: negative.

The optimized atomic geometries for the maximum number of hydrogen molecules adsorbed on one side of $\Theta = 0.50$ and $\Theta = 0.75$ Li coverage MoS_2 are shown in Fig. S4.

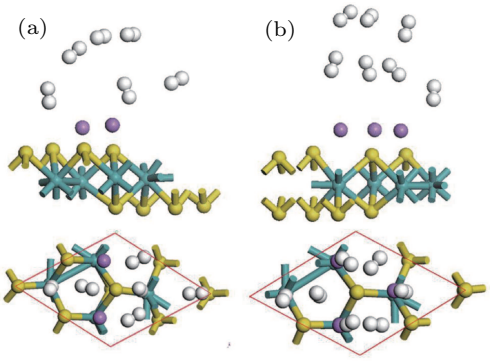


Fig. S4. (color online) The optimized atomic geometries for the maximum number of hydrogen molecules adsorbed on one side of $\Theta = 0.50$ and $\Theta = 0.75$ Li coverage MoS_2. Six hydrogen molecules can be adsorbed on one side of $\Theta = 0.50$ Li coverage MoS2, and seven hydrogen molecules can be adsorbed on $\Theta = 0.75$ Li coverage MoS_2.

The simulation snapshots of the hydrogen molecule dissociates on both sides of MoS_2 with the temperature set to 350 K are shown in Fig. S5.

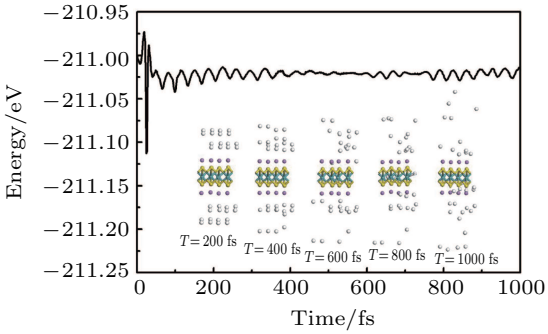


Fig. S5. (color online) Simulation snapshots of the hydrogen molecule dissociates on both sides of MoS_2 with the temperature set to 350 K. We carry this out for a 3-ps duration with a time step of 3 fs. One can see that only half of the adsorbed H_2 molecules can be dissociated and the dissociated H_2 molecules are in the atomic form. All that remained of the H_2 molecules is actually adsorbed in the molecular form. However, the binding energy is strong compared to that of the H_2 molecules adsorbed at 300 K.

References

[1] Schlapbach L and Zuttel A 2001 *Nature* **414** 353
[2] Rogner H H 1998 *Int. J. Hydrogen Energy* **23** 833
[3] Ataca C, Akturk E and Ciraci S 2009 *Phys. Rev. B* **79** 041406
[4] Wu J, Ong S M, Kang H C and Tok E S 2010 *J. Phys. Chem. C* **114** 21252
[5] Zhang C, Deng M S and Cai S H 2017 *Acta Phys. Sin.* **66** 128201 (in Chinese)
[6] Lee H, Ihm J, Cohen M L and Louie S G 2009 *Phys. Rev. B* **80** 115412
[7] Zhang Z, Zheng W and Jiang Q 2011 *Phys. Chem. Chem. Phys.* **13** 9483
[8] Yoon M, Yang S, Hicke C, Wang E, Geohegan D B and Zhang Z 2008 *Phys. Rev. Lett.* **100** 206806
[9] Huang L, Liu Y C, Gubbins K E and Nardelli M B 2010 *Appl. Phys. Lett.* **96** 063111
[10] Li M, Li J, Sun Q and Jia Y 2010 *J. Appl. Phys.* **108** 064326
[11] Zhao Y Q, Liu B, Yu Z L, Ma J, Wan Q, He P B and Cai M Q 2017 *J. Mater. Chem. C* **5** 5356
[12] Ley M B, Jepsen L H, Lee Y J, Cho Y W, Colbe J M V, Dornheim M, Rokni M, Jensen J O, Sloth M, Filinchuk Y, Jørgensen J E, Besenbacher F and Jensen T R 2014 *Mater. Today* **17** 122
[13] Cai M Q, Du Y and Huang B Y 2011 *Appl. Phys. Lett.* **98** 102907
[14] Durgun E, Ciraci S, Zhou W and Yildirim Y 2006 *Phys. Rev. Lett.* **97** 226102
[15] Cao D, Cai M Q, Hu W Y, Peng J, Zheng Y and Huang H T 2011 *Appl. Phys. Lett.* **98** 031910
[16] Cai M Q, Zheng Y, Wang B and Yang G W 2009 *Appl. Phys. Lett.* **95** 232901
[17] Sofo J O, Chaudhari A S and Barber G D 2007 *Phys. Rev. B* **75** 153401
[18] Ataca C, Akturk E, Ciraci S and Ustunel H 2008 *Appl. Phys. Lett.* **93** 043123
[19] Havu P, Ijäs M and Harju A 2011 *Phys. Rev. B* **84** 205423
[20] Sun Q, Wang Q, Jena P and Kawazoe Y 2005 *J. Am. Chem. Soc.* **127** 14582
[21] Liu W, Zhao Y, Li Y, Jiang Q and Lavernia E J 2009 *J. Phys. Chem. C* **113** 2028
[22] Zhang C, Geng X P, Tang S L, Deng M S and Du Y W 2017 *J. Mater. Chem. A* **5** 5912
[23] Zhang C, Lei C L, Cen C, Tang S L, Deng M S and Du Y W 2018 *Electrochim. Acta* **260** 814
[24] Meng S, Kaxiras E and Zhang Z 2007 *Nano Lett.* **7** 663
[25] Zhou C, Szpunar J A and Cui X 2016 *ACS Appl. Mater. Interfaces* **8** 15232
[26] Li H, Yin Z, He Q, Li H, Huang X, Lu G, Fam D W H, Tok A I Y, Zhang Q and Zhang H 2012 *Small* **8** 63
[27] Radisavljevic B, Radenovic A, Brivio J, Giacometti V and Kis A 2011 *Nat. Nanotechnol.* **6** 147
[28] Wu L J, Zhao Y Q, Chen C W, Wang L Z, Liu B and Cai M Q 2016 *Chin. Phys. B* **25** 107202

[29] Liu B, Wu L J, Zhao Y Q, Wang L Z and Cai M Q 2016 *J. Magn. Magn. Mater.* **420** 218
[30] Zhao Y Q, Wang X, Liu B, Yu Z L, He P B, Wan Q, Cai M Q and Yu H L 2018 *Org. Electron* **53** 50
[31] Kresse G and Hafner J 1993 *Phys. Rev. B* **47** 558
[32] Perdew J P, Burke K and Ernzerhof M 1996 *Phys. Rev. Lett.* **77** 3865
[33] Blochl P E 1994 *Phys. Rev. B* **50** 17953
[34] Kresse G and Joubert D 1999 *Phys. Rev. B* **59** 1758
[35] Kadantsev E S and Hawrylak P 2012 *Solid State Commun.* **152** 909
[36] Liu C, Li F, Ma L P and Cheng H M 2010 *Adv. Mater.* **22** E28
[37] Liu C, Fan Y Y, Liu M, Cong H T, Cheng H and Dresselhaus M S 1999 *Science* **286** 1127
[38] Putungan D B, Lin S, Wei C and Kuo J 2015 *Phys. Chem. Chem. Phys.* **17** 11367
[39] Suh M P, Park H J, Prasad T K and Lim D 2009 *Chem. Soc. Rev.* **38** 1294
[40] Chan K T, Neaton J B and Cohen M L 2008 *Phys. Rev. B* **77** 235430
[41] Wu X, Yang J and Zeng X C 2006 *J. Chem. Phys.* **125** 44704
[42] Lee H, Ihm J, Cohen M L and Louie S G 2010 *Nano Lett.* **10** 793
[43] Zhang C, Wei J, Chen L, Tang S L, Deng M S and Du Y W 2017 *Nanoscale* **9** 15423
[44] Zhang C, Huang Y, Tang S L, Deng M S and Du Y W 2017 *ACS Energy Lett.* **2** 759